*Natural Resources Research, Vol. 33, No. 2, April 2024 (© 2024)*
https://doi.org/10.1007/s11053-023-10300-6

*Original Paper*

# Effect of Mean Specific Gravity on Combustion Characteristics of Selected High Ash Indian Coal

**Dibyajyoti Behera,[1] Pritam Kumar,[1] and Barun Kumar Nandi[1,2]**

*Received 31 August 2023; accepted 23 December 2023*
*Published online: 29 January 2024*

The present research shows the combustion characteristics of different specific gravity fractions of high ash thermal coal. Coal with different mean specific gravity ($SG_M$) ranging from 1.25 to 2.0 was produced using the float–sink experiment. All $SG_M$ coals were characterized with proximate analysis, ultimate analysis, higher heating value, ash analysis, Brunauer–Emmett–Teller analysis and Fourier-transform infrared spectroscopy (FTIR). Combustion experiments were performed with thermogravimetric analysis to identify the impact of $SG_M$. Experimental results inferred that ignition temperature ranged from 285 to 408 °C as $SG_M$ varied from 1.25 to 2.0. The combustion rate of 1.25 $SG_M$ coal was found to be the highest due to the strong or moderate presence of hydrocarbons like alkane, alkene, aldehyde and alcoholic, as observed from FTIR. Activation energy ranged from 121.81 to 54.60 kJ/ mol as $SG_M$ of coal increased from 1.25 to 2.0. Thermodynamic analysis inferred that 1.65 $SG_M$ coal had the highest ΔS (− 158.21 J/mol. K) and minimum ΔH (48.93 kJ/ mol), inferring ease of decomposition and higher combustion reactivity.

**KEY WORDS:** Coal, Combustion, Mean specific gravity, Activation energy, Thermodynamic analysis.

## INTRODUCTION

Developing countries depend mainly on coal for electricity generation, as coal in such countries is an affordable, cheap, secure and efficient power source for its growing economy. Due to continuous electricity demand, coal will remain one of the prime energy sources for upcoming decades due to the minimal coal price and low operational cost of thermal power plants compared to renewable-based power plants. Coal compositions and properties vary depending on the extent of alternation or degree of coalification of the original plant material from which they were derived (Wang et al., 2022). Proximate analysis (PRA), ultimate analysis (ULA) and higher heating value (HHV) evaluation are the primary characterization methods for coal. Heat release rate is also an essential parameter for the combustor design of thermal power plants. Substantial heat release over a short period of time might damage boiler tubes and worsen slagging properties of ash, and so coal with high heat release rate and low HHV is not preferred. Similarly, coal with low heat release rate and high HHV is undesirable because it might not produce steam of the necessary quality (Liu et al., 2020). Hence, coal with the desired heat release rate and HHV is essential for thermal utilities. Coal's heat release rate depends mainly on the chemical reactivity between coal hydrocarbons and supplied oxygen. Such combustion reactivity also depends on the surface characteristics of coal and different functional groups present as hydrocarbons, usually represented as

[1]Department of Fuel Minerals and Metallurgical Engineering, Indian Institute of Technology (Indian School of Mines), Dhanbad, Jharkhand 826004, India.
[2]To whom correspondence should be addressed; e-mail: barun@iitism.ac.in



1520-7439/24/0400-0727/0 

combustible matter in coal. Fixed carbon (FC), volatile matter (VM) and ULA parameters are commonly used to describe the quality and quantity of various hydrocarbons in coal. In coal, the hydrocarbons are primarily made of hydrogen, carbon, oxygen and other minor elements, including sulfur and nitrogen. Depending on the bond strength between these elements, coal's hydrocarbons react with oxygen in different ways, and accordingly, the heat release rate varies. These coal characteristics can vary significantly among mines in the same coalfield and different seams within the same mine. Therefore, knowledge of coal's internal structure is required before burning coal in a boiler.

Thermal power stations buy coal based on their HHV. Regulations of different countries state that coal from various sources, including seams, multiple sites and imported coal, is traded on the same level without considering its natural combustion properties (Tiwari et al., 2015). The effectiveness of the combustion process for pulverized coal depends on how well coal of different specific gravity mixes with the primary air brought in from the outside. Based on coal's specific gravity and particle size, air flow rate control systems are created for this process so that coal particles properly mix with air without settling down or going outside of the reactor (Nag, 2014). It is challenging to burn other types of coal with a combustor once it has been designed for a specific type of coal. Coal from other sources having different HHV and specific gravity will be unable to produce the required heat to keep the steam quality at the proper temperature and pressure, which is vital for plant operation. A similar observation for the combustion of different specific gravity coal was made by Lv et al. (2020). They conveyed that with the variation of specific gravity, coal's HHV varies due to mineral matter variation and combustible hydrocarbon availability in coal. Fortish et al. (2000) found that the specific gravity of coal particles significantly affect coal combustion characteristics. Until now, very little work has been reported by scientists to establish directly the correlation between coal specific gravity or ash with coal combustion behavior. Wu et al. (2019) found that the specific gravity of coal is critical for size segregations in pulverized coal combustion. Zhang et al. (2015) found that functional groups, such as aliphatic alkane, alkene, aromaticity, alcoholic groups, phenolic groups, in coal varies with change in coal rank. As a consequence, the combustion performance of coal fluctuates significantly based on their rank. Cao et al. (2015) observed that the availability of functional groups changes with coal particle size. Shen et al. (2018) reported combustion characteristics and flu gas composition varied significantly with change in coal's functional groups during combustion and pyrolysis. Song et al. (2017) studied coal combustion characteristics using TG–FTIR (thermogravimetry—Fourier-transform infrared spectroscopy). They observed that $CH_4$ and $CO_2$ release varied largely with change in the presence of aliphatic chain and carboxyl groups. Sarkar et al. (2013) identified the combustion characteristics of coals using TGA (thermogravimetric analysis) and reported that high ash coal has inferior ignition temperature ($T_{IN}$), peak temperature ($T_{PK}$) and burnout temperature ($T_{FL}$) than low ash coal. Using TGA, Biswas et al. (2006) investigated the combustion behavior of two coal of same rank but with different ash content. They reported that high ash coal has poor $T_{PK}$ and $T_{FL}$ compared to low ash coal. Banerjee et al. (2016) estimated the variation in combustible materials, mineral compositions and ash fusibility of four coal samples collected from the different seams of the same coal mine. They found considerable variation in FC and VM with depth of seam. Mineral compositions, such as $SiO_2$, $Al_2O_3$, CaO, $TiO_2$ and $Fe_2O_3$, are almost identical, and all coals' slagging and fouling nature are on the lower side. Kumari et al. (2016) investigated the role of mineral composition during the use of coal in thermal utilities and reported that $SiO_2$ is the predominant mineral in Indian coal. Saini and Srivastava (2017) analyzed slagging and fouling behavior of different specific gravity fractions of coal. They found that slagging and fouling characteristics are higher for heavier specific gravity coal fractions due to high ash content and alkaline minerals. Yu et al. (2020) analyzed the impact of surface porosity on the combustion characteristics of coal. They conveyed that pore provides a good passage for $O_2$ to the coal surface, which improves combustion performance. Mishra (2022) found that exposure to greater surface area leads to higher oxygen diffusion into coal, which increases combustibility. Wang et al. (2018) studied the role of surface morphology on coal combustion characteristics using FESEM (field emission scanning electron microscopy) and TGA. They found that coal has combustion difficulty and requires higher activation energy due to the inferior texture of coal particles.

Earlier reports by other scientists infer that coal combustion is a sophisticated phenomenon, affected significantly by the surface properties of coal and hydrocarbons, functional groups, and inorganic mineral matter available in coal. The coal conversion rate is generally modified by altering turbulence in the combustion chamber due to the large variation in the specific gravity of coal with mineral matter quantity and composition (Gupta, 2007). Hence, a relation between coal properties and specific gravity associated with coal combustion characteristics must be established to utilize coal effectively. Generally, power plants have only PRA and HHV data available, whereas various important characteristics such as functional groups, surface characteristics, hydrocarbon types and mineral matter composition for coal are unavailable. Due to the unavailability of such crucial information, most thermal utilities increase the coal feed rate in the burner to maintain the required heat release rate. As a result, unburned coal particles and combustible gases increase in the exhaust gas. Thus, characterization such as PRA, ULA, FESEM, FTIR, ash analysis and Brunauer–Emmett–Teller (BET) analysis is essential to identify the effect of combustible and non-combustible matter, surface texture, different functional groups and mineral compositions on the combustion behavior of coal particles with different densities. Apart from those, analyses of ash slagging characteristics, enthalpy, Gibbs energy and entropy during combustion are also necessary to identify the variation of endothermicity, decomposition difficulty and nature of the reaction during the combustion of different specific gravity coal. Studies on this issues are limited until now. Hence, the major objective of this work was to develop a relation between coal's combustion characteristics and its specific gravity or ash in order to optimize coal selection for efficient combustion characteristics in thermal power plants.

To achieve the objectives of the present research, coal of different specific gravity fractions represented by mean specific gravity ($SG_M$) ranging from 1.25 to 2.0 were prepared using the float–sink separation method. Prepared coals were characterized by PRA, ULA and HHV. Different hydrocarbons present as functional groups in coal were identified with FTIR. FESEM was done to identify the surface structure. Simultaneously, BET analysis was performed to explore the impact of surface porosity on coal combustion characteristics. Combustion experiments of coal with different $SG_M$ were performed using TGA to extract critical combustion characteristics parameters. The heat release, coal consumption and ash generation rates with variation of coal $SG_M$ were also analyzed. Further, kinetic and thermodynamic parameters were determined to get more insight into the combustion reaction.

## EXPERIMENTAL METHODOLOGY

Sub-bituminous coal of about 150 kg was collected from the Kajora mines, Eastern Coalfields Limited, West Bengal, India. The coal samples were brought in air-tight plastic bags to the institute's coal preparation laboratory within two days of collection. After that, the entire coal samples were crushed to $-$ 50 + 0.5 mm using a conical crusher, jaw crusher and roll crusher. Later, coal particles produced by crushing were thoroughly mixed to obtain a uniform mixture of coal. The float–sink experiments were performed by the blending of organic liquids such as bromoform (specific gravity: 2.90), trichloroethylene (specific gravity: 1.45) and kerosene (specific gravity: 0.80) in the required volume proportion to prepare specific gravity solutions ranging from 1.25 to 1.90. The specific gravity of all fractions of the solution was estimated using a hydrometer. $SG_M$ between 1.25 and 2.0 was estimated by the arithmetic mean of each specific gravity fraction of coal. After float–sink experiment, coal of each specific gravity fraction was cleaned with tap water and then dried. About 300 gm of prototypical coal samples of $-$ 72 mesh sizes were made by following the size decrement and sampling as per the standard procedure (Cai et al., 2021). All specific gravity fractions of coal were characterized with different characterization methods, namely, PRA (A.S.T.M D3173); HHV analysis with bomb calorimeter (Make: LECO; Model: AC 350); ULA with CHNS analyzer (Make: Vario; Model: III); BET analysis (Make: Micromeritics Instrument Corporation; Model: 3FLEX 3500); surface morphology with FESEM (Make: Supra'55; Model: Mono CL4); XRF (Make: Burker; Model: S8 Tiger). Combustion experiments were done using TGA (Make: NETZSCH; Model: STA449 F3 Jupiter). For the combustion experiment, about 15–20 mg of coal was kept in TGA crucible and was non-isothermally heated at 10 °C/min in the presence of pure $O_2$ with a 60 ml/min flow rate. Using TGA data, a number of combustion associated parameters, namely, initiation temperature ($T_{IN}$), burnout temperature ($T_{FL}$), maximum temperature ($T_{PK}$) and maximum combustion rate ($DTG_{peak}$) (mass %/min) were calculated (Aich et al., 2019).

After that, important performance indices, namely, initiation index ($I_{IN}$), characteristics index ($C_{IN}$), burnout index ($B_{IN}$) and heat intensity index ($H_{IN}$) were determined using the following equations (Aich et al., 2019; Chakraborty et al., 2021):

$$I_{IN} = \frac{DTG_{peak}}{t_{IN} \times t_{PK}} \quad (1)$$

$$C_{IN} = \frac{DTG_{peak} \times DTG_{mean}}{T_{IN}^2 \times T_{FL}} \quad (2)$$

$$B_{IN} = \frac{DTG_{peak}}{t_{PK} \times t_{FL} \times \Delta t_{1/2}} \quad (3)$$

$$H_{IN} = T_{PK} \times \ln\left(\frac{\Delta T_{1/2}}{DTG_{Peak}}\right) \times 10^{-3} \quad (4)$$

where $t_{IN}$, $t_{PK}$, $t_{FL}$ are times corresponding to $T_{IN}$, $T_{PK}$, $T_{FL}$, while $\Delta t_{1/2}$ is time associated with $DTG/DTG_{peak} = 0.5$, $DTG_{mean}$ is the average combustion rate during the entire reaction. Activation energy ( $E_C$) and pre-exponential factor ($f$) during combustion were estimated by the Coats–Redfern (CR) method (Nyoni et al., 2020; Zou et al., 2022), thus:

$$\ln\frac{-\ln(1-\varphi)}{T^2} = \ln\left(\frac{f \times R}{\lambda \times E_C}\left[1 - \left(\frac{2R \times T}{E_C}\right)\right]\right) - \frac{E_C}{R \times T} \quad (5)$$

where $\varphi$ is fuel conversion, $\lambda$ is heating rate, $E_C$ is activation energy in kJ/mol, $f$ is pre-exponential factor in $sec^{-1}$, R is the universal gas constant (8.314 J/K mol), T is temperature (K). Change in thermodynamic parameters, namely, enthalpy ($\Delta H$), Gibbs free energy ($\Delta G$) and entropy ($\Delta S$) were estimated respectively as (Mishra et al., 2020; Merdun & Laouge, 2021):

$$\Delta H = E_C - R \times T_{PK} \quad (6)$$

$$\Delta G = E_C + R \times T_{PK} \times \ln\left(\frac{\Psi \times T_{PK}}{\varepsilon \times f}\right) \quad (7)$$

$$\Delta S = \frac{\Delta H - \Delta G}{T_{PK}} \quad (8)$$

where $\Psi$ is Boltzmann constant ($1.3806 \times 10^{-23}$) and $\varepsilon$ is the Planck constant ($6.626 \times 10^{-34}$).

## RESULTS AND DISCUSSIONS

### Impact of $SG_M$ on Coal Properties

The variations in proximate and ultimate analysis, HHV and fuel ratio based on dry ash free basis along with weight distribution corresponding to the head sample and each $SG_M$ of coal are shown in Table 1. From Table 1, head coal sample had lower ash (20.21%) but higher VM (46.30%) and FC (77.20%) compared to typical high ash Indian coal (ash: 29–40%; VM: 20–30%; FC: 23–53%) (Raghuvanshi et al., 2022). Similarly, C (77.20%), H (8.24%), S (2.67%) and N (2.05%) were on the higher side. From Table 1, it is observed that, as $SG_M$ of coal increases from 1.25 to 2.0, ash deteriorates from 2.41 to 76.36%, VM changes from 46.30

**Table 1.** Fluctuations in physical–chemical properties, HHV and fuel ratio* of coal with $SG_M$

| Specific gravity range | $SG_M$ | Weight (%) | Proximate analysis (%) | | | | Ultimate analysis (%)* | | | | | Fuel ratio* (FC/VM) | HHV* (kcal/kg) |
|---|---|---|---|---|---|---|---|---|---|---|---|---|---|
| | | | Ash | Moisture | V.M* | F.C* | C | H | S | N | O | | |
| Head coal | – | 100 | 20.21 | 4.89 | 46.30 | 66.56 | 77.20 | 8.24 | 2.67 | 2.05 | 9.84 | 1.44 | 9000 |
| 1.25 < SG | 1.25 | 0.61 | 2.41 | 8.56 | 42.70 | 57.30 | 79.64 | 6.29 | 0.66 | 2.21 | 11.20 | 1.34 | 9606 |
| 1.25 < SG < 1.3 | 1.275 | 20.63 | 6.76 | 7.32 | 44.60 | 55.40 | 78.56 | 6.40 | 0.64 | 2.27 | 12.13 | 1.24 | 9440 |
| 1.3 < SG < 1.35 | 1.325 | 22.55 | 11.56 | 6.46 | 45.51 | 54.48 | 78.31 | 6.46 | 0.61 | 2.27 | 12.34 | 1.19 | 9316 |
| 1.35 < SG < 1.4 | 1.375 | 24.16 | 16.77 | 5.53 | 45.33 | 54.67 | 77.61 | 6.18 | 0.59 | 2.21 | 13.41 | 1.20 | 9166 |
| 1.4 < SG < 1.45 | 1.425 | 3.93 | 21.32 | 4.94 | 43.42 | 56.58 | 76.21 | 5.97 | 0.60 | 2.28 | 14.94 | 1.30 | 9057 |
| 1.45 < SG < 1.5 | 1.475 | 11.57 | 26.79 | 5.37 | 44.53 | 55.60 | 75.18 | 5.75 | 0.56 | 2.36 | 16.16 | 1.25 | 9102 |
| 1.5 < SG < 1.6 | 1.55 | 3.73 | 27.24 | 4.46 | 42.58 | 57.42 | 68.08 | 5.42 | 0.57 | 2.17 | 23.76 | 1.24 | 8944 |
| 1.6 < SG < 1.7 | 1.65 | 3.03 | 37.49 | 4.15 | 45.05 | 54.95 | 62.71 | 5.48 | 0.60 | 2.07 | 29.13 | 1.22 | 8801 |
| 1.7 < SG < 1.8 | 1.75 | 2.67 | 48.14 | 4.00 | 48.43 | 51.57 | 68.32 | 5.64 | 0.61 | 2.51 | 22.92 | 1.06 | 8627 |
| 1.8 < SG < 1.9 | 1.85 | 5.27 | 55.16 | 3.57 | 53.19 | 46.81 | 61.55 | 5.33 | 0.65 | 2.54 | 29.92 | 0.88 | 8379 |
| SG > 1.9 | 2.0# | 1.40 | 76.36 | 2.02 | 66.70 | 33.35 | 53.65 | 6.48 | 0.60 | 3.38 | 35.89 | 0.50 | 6577 |

#Standard methods were used to determine coal mean specific gravity (Gupta, 2000). *Dry ash free basis to 66.70% and FC declines from 66.56 to 33.35%. Such changes can be described by the fact that FC's specific gravity is lighter than mineral matter's. Thus, with rise in coal $SG_M$, mineral matter represented by ash content rises while carbonaceous content reduces, FC declines, while VM also remarkably changes. Such observations are further verified with the ULA, indicating that C deteriorates from 79.64 to 53.65% and H changes from 5.33 to 6.48% as $SG_M$ rise from 1.25 to 2.0. Coal with 1.25 $SG_M$ had the highest fuel ratio 1.34. Fuel ratio declined from 1.34 to 0.5 as $SG_M$ rose from 1.25 to 2.0. Such reduction in fuel ratio with $SG_M$ can be attributed to substantial reduction in FC and rise in VM of coal. Table 1 shows that HHV of 1.25 $SG_M$ coal was maximum (9606 kcal/kg). Further, HHV reduced from 9606 to 6577 kcal/kg as coal $SG_M$ rose from 1.25 to 2.0. Such investigations are consistent with the decline of C and O contents in coal as $SG_M$ increases, reducing coal's combustibles and oxidative environment. Therefore, availability of energy density in coal declines as $SG_M$ increases.

## Impact of $SG_M$ on FTIR

Fluctuations in functional groups with the change in coal $SG_M$ were investigated with FTIR. Figure 1a–b depicts functional groups and corresponding peaks extracted from FTIR and results are summarized in Table 2. Figure 1a–b and Table 2 illustrate notable deviations in the bond intensity of functional groups for different wavelengths with the variation in $SG_M$ of coals. Peaks in 3700–3600 $cm^{-1}$ associated with O–H bond for alcoholic functional groups were absent in 1.25–1.375 $SG_M$ coal, weak in 1.425 and 1.475 $SG_M$ coal, while strong for 1.55 to 2.0 $SG_M$ coal (Chakravarty et al., 2020). This infers that hydrocarbon-rich alcoholic functional groups increase with rise in coal $SG_M$. Peaks between 3450 and 3350 $cm^{-1}$ related with N–H group for prime amines were stronger for 1.25–1.375 $SG_M$ coal, moderate for 1.425 and 1.475 $SG_M$ coal and mild for 1.55–2.0 $SG_M$ coal (Odeh, 2015). Such observation implies that prime amines enriched hydrocarbons reduce in coal when coal $SG_M$ increases. Similarly, peak of C–H group associated with aliphatic $CH_3$ and aliphatic $CH_2$ asymmetric stretching vibration between 3000–2800 $cm^{-1}$ wavelength were found mild for 1.65–2.0 $SG_M$ coal, moderate for 1.475–1.55 $SG_M$ coal and strong for 1.25–1.425 $SG_M$ coal (Xuguang 2005; Chakravarty et al., 2020). This shows that, with increase in $SG_M$, aliphatic rich hydrocarbon reduces. Similar examinations were also seen for aromatic nucleus associated with C=C stretching at 1650–1500 $cm^{-1}$ and were stronger for 1.25–1.375 $SG_M$ coal and moderate for 1.425–2.0 $SG_M$ coal (Mishra et al., 2016a). The above finding infers that all SG fractions of coal contain aromatic C = C ring, decreasing with increase in coal $SG_M$. Peaks around 1500–1400 $cm^{-1}$ for aliphatic chain of C–H band associated with alkanes and aldehyde were moderate for 1.25–1.425 $SG_M$ coal, weak for 1.475–1.55 $SG_M$ coal and absent for 1.65–2.0 $SG_M$ coal (Odeh, 2015; Mishra et al., 2016a). The C–O–C stretching corresponding to anhydride hydrocarbons within 1050–1000 $cm^{-1}$ was present in all $SG_M$ coal, signifying all coals have anhydride compounds (Wang et al., 2016).

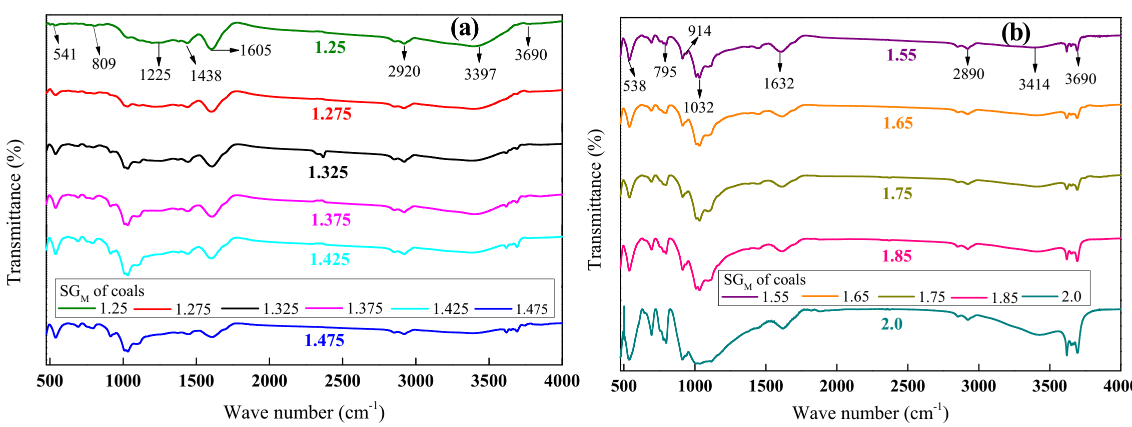


**Figure 1.** (**a–b**) Variation in functional groups with different $SG_M$ coal..

**Table 2.** Functional group fluctuations with $SG_M$ coal

| Wavenumber ($cm^{-1}$) | Functional group | $SG_M$ | | | | | | | | | | |
|---|---|---|---|---|---|---|---|---|---|---|---|---|
| | | 1.25 | 1.275 | 1.325 | 1.375 | 1.425 | 1. 475 | 1.55 | 1.65 | 1.75 | 1.85 | 2.0 |
| 3700–3650 | O–H stretching, alcohol | – | – | – | W | W | W | S | S | S | S | S |
| 3450–3350 | O–H Stretching alcohol/ N–H stretching primary amine | S | S | S | S | M | M | W | W | W | W | W |
| 3000–2800 | Aliphatic C–H stretching, alkane | S | S | S | S | S | M | M | W | W | W | W |
| 1650–1500 | Aromatic nucleus C=C stretching and C=O stretching alkene | S | S | S | S | M | M | M | M | M | M | M |
| 1500–1400 | Aliphatic chains of C–H bending, aldehyde, alkane | M | M | M | M | M | W | W | - | - | - | - |
| 1050–1000 | Silicates (Si–O), C−O−R and C−O structures | – | W | M | S | S | S | S | S | S | S | S |
| 970–900 | C=C bending, alkene | – | – | – | – | M | M | M | M | M | S | S |
| 800–750 | C=C bending, alkene (tri-substituted) | W | W | W | W | M | M | S | S | S | S | S |
| 550–475 | C–I stretching, halo compound | W | W | M | M | S | S | S | S | S | S | S |

*S Strong, M Moderate, W Weak/mild

Peaks at 970–900 $cm^{-1}$ for C=C stretching related to alkenes were absent for 1.25–1.375 $SG_M$ coal but were available with moderate to strong intensity for 1.425–2.0 $SG_M$ coal; inferring lighter $SG_M$ coal has unavailability of C=C bond for alkene hydrocarbons. Peaks at 800–750 $cm^{-1}$ associated with C=C stretching of alkene (tri-substituted) hydrocarbons were very strong in 1.55–2.0 SGM coal and present moderate or weak peaks for all other $SG_M$ coal. Peaks at 550–450 $cm^{-1}$ associated with C–I peak corresponding to halogen compounds were weak for 1.25–1.275 $SG_M$, moderate for 1.325–1.375 $SG_M$ and strong for 1.425–2.0 $SG_M$ coal. Overall, results obtained from FTIR showed that O–H bonding related to alcoholic hydrocarbons, C=C stretching for tri-substituted alkene and C–H stretching due to aldehyde are weakly present or nonexistent in 1.25–1.375 $SG_M$ coal although they are strongly present in 1.55–2.0 $SG_M$ coal and moderately or mildly present in 1.425 and 1.475 $SG_M$ coal. Thus, different $SG_M$ coal consists of various hydrocarbons and will impact coal combustion performance accordingly.

## Impact of $SG_M$ on Surface Morphology and Pore Characteristics

Figure 2 illustrates the variation in surface morphology with coal $SG_M$. Figure 2 shows 1.25 SGM coal has more longitudinal cracks than heavier density fraction coals. Such cracks promote the diffusion of gases and consequently lower endothermic energy is required for the conversion of various functional groups, such as C=C tri-substituted alkenes (800–750 $cm^{-1}$), alkene (970–900 $cm^{-1}$), aliphatic chains of CH bending such as aldehyde and alkane (1500–1400 $cm^{-1}$), aliphatic-$CH_2$ and -$CH_3$ stretching (3000–2800 $cm^{-1}$) and alcoholic/prime amine group (3400–3350 $cm^{-1}$), of 1.25 $SG_M$ coal into various intermediate products and finally to $H_2O$ and $CO_2$ (Wang et al., 2016; Kumar and Nandi 2021). Coals with 1.275 and 1.325 $SG_M$ show good porous texture, promoting their reactivity, while heavier SGM coals have less porous or non-porous texture. Such inferior porous morphology signifying larger decomposition energy would be required for the conversion of heavier $SG_M$ coals into end products, and, as a result, the combustion of such coals in power plants are challenging, as the use of such coals may damage the boiler tubes of different sections due to significant deviation in heat received by boiler tubes from the designed values.

BET analysis (adsorption isotherm) was carried out to gain better insights to coal surface texture with variation in coal $SG_M$. Pore characteristic parameters such as mean pore size, specific surface area and pore volume with varying coal $SG_M$ were obtained and shown in Table 3. Table 3 shows that the mean pore size of coal fluctuated significantly as coal specific gravity varied. Lighter $SG_M$ coals, namely 1.25, 1.275, 1.325, 1.375 and 1.475 showed relatively larger pore sizes than heavier $SG_M$ coal such as 1.425, 1.55, 1.65, 1.75 and 1.85. Such varia-

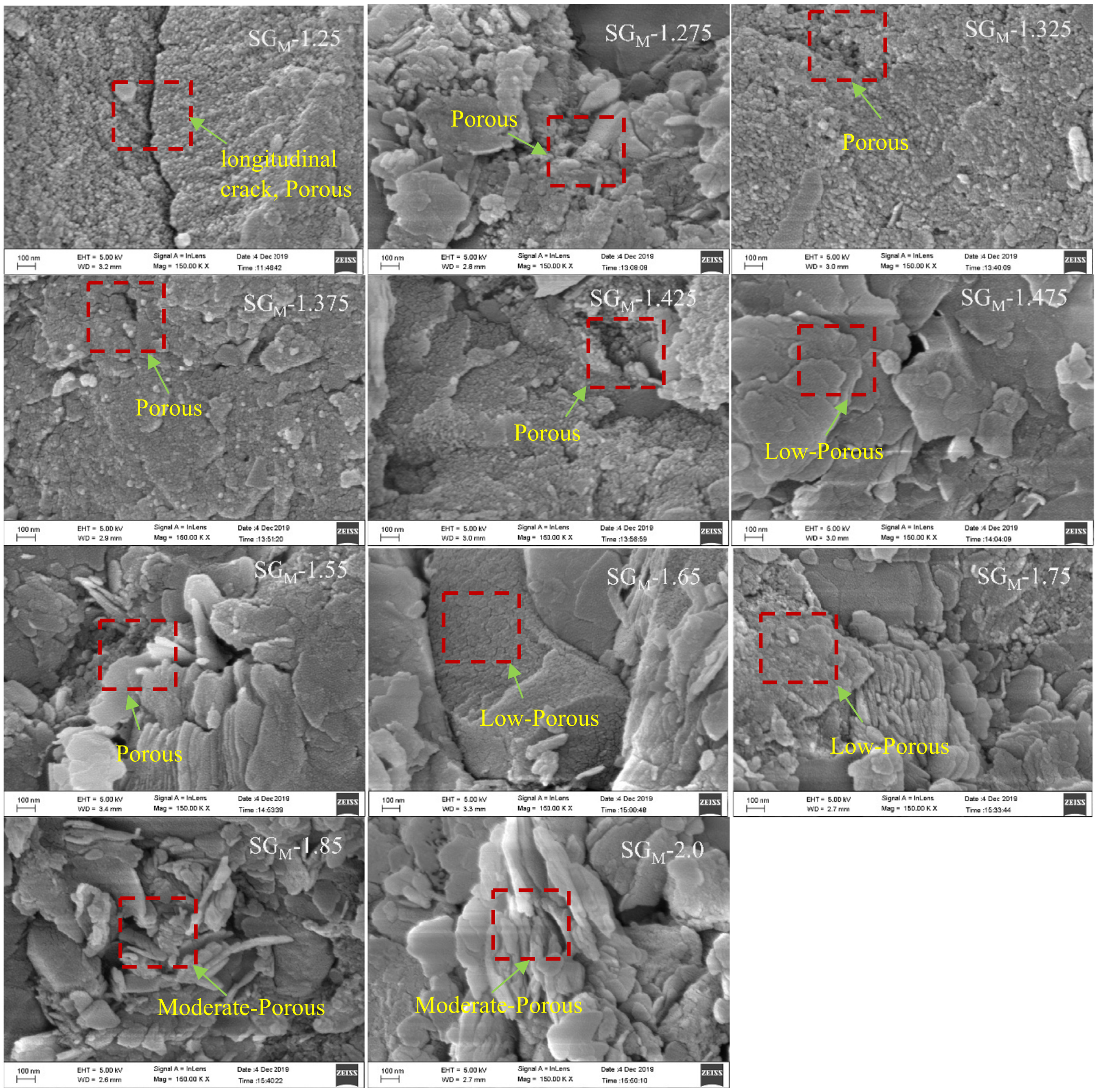


**Figure 2.** FESEM images of different $SG_M$ coal..

**Table 3.** Variation of mean pore size, specific surface area and total pore volume with the variation of coal $SG_M$

| Surface properties | $SG_M$ | | | | | | | | | | |
|---|---|---|---|---|---|---|---|---|---|---|---|
| | 1.25 | 1.275 | 1.325 | 1.375 | 1.425 | 1. 475 | 1.55 | 1.65 | 1.75 | 1.85 | 2.0 |
| Mean pore size (nm) | 10.67 | 22.01 | 23.87 | 12.57 | 4.46 | 12.70 | 8.11 | 7.96 | 7.0 | 7.86 | 10.05 |
| Specific surface area ($m^2/g$) | 2.97 | 1.60 | 1.78 | 13.31 | 256.36 | 60.14 | 93.39 | 117.20 | 173.51 | 147.06 | 59.79 |
| Total pore volume $\times 10^{-4}$ ($cm^3/g$) | 1.77 | 2.51 | 2.31 | 33.94 | 55.68 | 20.42 | 29.62 | 37.21 | 54.78 | 29.41 | 8.43 |

tions across different $SG_M$ coals are attributed to availability or unavailability of different kinds of functional groups, such as C=C tri-substituted alkenes, alkene, aromatic aldehyde/alkane, aliphatic-$CH_2$/-$CH_3$ stretching and alcoholic/prime amine group, and variation in distributions of combustible

**Table 4.** Variation in ash constituents (in mass%) with $SG_M$ of coal

| $SG_M$ | 1.25 | 1.275 | 1.325 | 1.375 | 1.425 | 1.475 | 1.55 | 1.65 | 1.75 | 1.85 | 2.0 |
|---|---|---|---|---|---|---|---|---|---|---|---|
| $SiO_2$ | 46.72 | 49.82 | 53.29 | 55.30 | 55.85 | 58.60 | 62.73 | 59.49 | 57.99 | 42.37 | 48.21 |
| $Al_2O_3$ | 24.30 | 25.66 | 25.51 | 25.08 | 25.68 | 27.34 | 23.04 | 24.30 | 25.92 | 1.49 | 5.47 |
| MgO | 3.17 | 3.01 | 2.79 | 2.65 | 2.61 | 2.55 | 2.58 | 2.60 | 2.49 | 42.71 | 16.12 |
| $Fe_2O_3$ | 6.78 | 5.36 | 4.02 | 3.28 | 3.06 | 2.94 | 2.62 | 3.55 | 3.08 | 8.54 | 10.12 |
| $TiO_2$ | 2.15 | 1.97 | 1.87 | 1.77 | 1.70 | 1.69 | 1.57 | 1.58 | 1.56 | 0.00 | 0.64 |
| MnO | 0.08 | 0.08 | 0.08 | 0.07 | 0.07 | 0.07 | 0.07 | 0.08 | 0.09 | 0.10 | 0.14 |
| CaO | 2.56 | 2.68 | 1.93 | 1.33 | 0.82 | 0.51 | 0.37 | 0.35 | 0.70 | 0.73 | 14.97 |
| $Na_2O$ | 0.31 | 0.27 | 0.27 | 0.25 | 0.25 | 0.25 | 0.24 | 0.25 | 0.25 | 0.43 | 0.69 |
| $K_2O$ | 1.48 | 1.51 | 1.59 | 1.71 | 1.81 | 1.95 | 2.08 | 2.02 | 1.70 | 0.01 | 0.55 |
| $P_2O_5$ | 0.73 | 0.79 | 0.59 | 0.38 | 0.22 | 0.13 | 0.08 | 0.08 | 0.06 | 0.03 | 0.11 |
| $Cr_2O_3$ | 0.46 | 0.46 | 0.46 | 0.47 | 0.46 | 0.48 | 0.46 | 0.76 | 0.46 | 0.57 | 0.45 |

**Table 5.** Variation in slagging and fouling parameters with SGM of coal

| SGM | 1.25 | 1.275 | 1.325 | 1.375 | 1.425 | 1.475 | 1.55 | 1.65 | 1.75 | 1.85 | 2.0 |
|---|---|---|---|---|---|---|---|---|---|---|---|
| $R_{BA}$ | 0.19 | 0.17 | 0.13 | 0.11 | 0.10 | 0.09 | 0.09 | 0.10 | 0.09 | 1.19 | 0.78 |
| $F_{IT}$ | 0.35 | 0.29 | 0.24 | 0.22 | 0.22 | 0.21 | 0.21 | 0.23 | 0.18 | 0.53 | 0.97 |
| $S_{RT}$ | 0.79 | 0.82 | 0.86 | 0.88 | 0.89 | 0.91 | 0.92 | 0.90 | 0.90 | 0.44 | 0.53 |

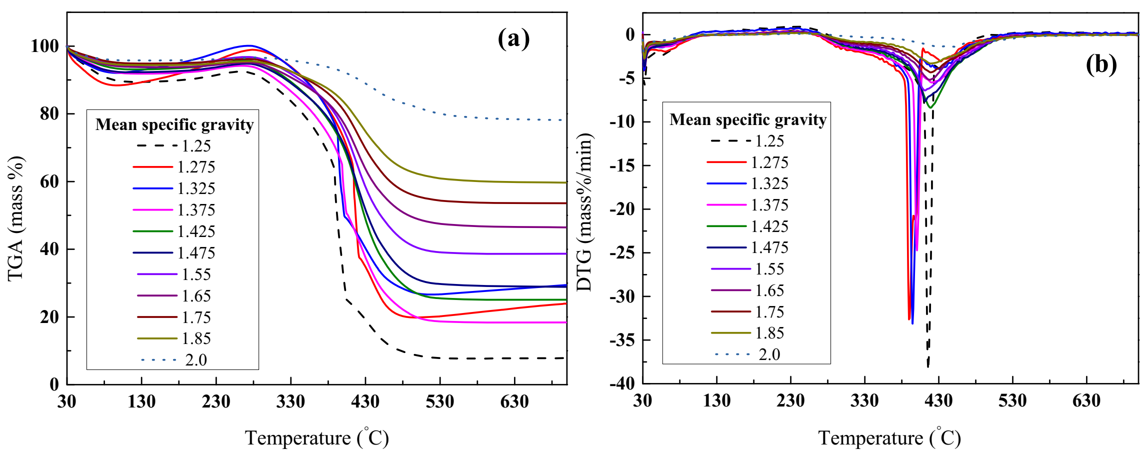


**Figure 3.** TGA–DTG profiles for combustion of different $SG_M$ coal..

and mineral matters across different $SG_M$ of coal (Sampath et al. 2020; Fang et al., 2022). Overall, it can be concluded that 1.425 $SG_M$ coal had the smallest pore size of 4.46 nm, and the highest pore volume of $55.68 \times 10^{-4}$ (cm$^3$/g) and surface area of 256.36 m$^2$/g. The presence of such higher surface area and pore volumes in 1.425 $SG_M$ coal will ease the diffusion of gases and consequently, lower decomposition energy is required for the conversion of functional groups into various intermediate products and finally to $H_2O$ and $CO_2$ (Wang et al., 2016; Kumar and Nandi 2021). Thus, it is expected that 1.425 $SG_M$ coal will ignite easily compared to other $SG_M$ coal during combustion. Table 3 shows that the specific surface area increased with $SG_M$ of coal. Such improvement in surface area may be attributed to the rise of inorganic mineral oxides such as MgO, $Fe_2O_3$, CaO and $Na_2O$ (as shown in Table 4) in coal (Sun et al., 2013). As inorganic matter constitutes different inorganic salts, they are rela-

**Table 6.** Changes in combustion profile parameters with the variation of coal $SG_M$

| Coal $SG_M$ | | | | $T_{IN}$(°C) | $T_{PK}$(°C) | $T_{FL}$(°C) | $DTG_{Peak}$(mass%/min) | |
|---|---|---|---|---|---|---|---|---|
| | | | | $I_{IN} \times 10^{-3}$ (mass/min$^3$) | $C_{IN} \times 10^{-8}$ (mass$^2$/min$^2$ °C$^3$) | $B_{IN} \times 10^{-5}$(mass/min$^4$) | $H_{IN}$(°C) | |
| 1.25 | 303 | 415 | 472 | 38.5 | 38.1 | 101.1 | 76.4 | 0.9 |
| 1.275 | 285 | 398 | 469 | 21.2 | 23.5 | 65.7 | 53.9 | 1.0 |
| 1.325 | 294 | 394 | 479 | 33.1 | 35.9 | 97.3 | 72.8 | 0.9 |
| 1.375 | 288 | 400 | 494 | 24.7 | 27.1 | 74.5 | 57.3 | 1.0 |
| 1.425 | 294 | 418 | 497 | 8.3 | 8.5 | 23.2 | 13.2 | 1.6 |
| 1.475 | 296 | 411 | 495 | 7.6 | 7.8 | 21.1 | 12.4 | 1.6 |
| 1.55 | 303 | 411 | 492 | 6.3 | 6.4 | 16.9 | 10.6 | 1.7 |
| 1.65 | 309 | 417 | 490 | 5.1 | 5.0 | 13.0 | 8.5 | 1.8 |
| 1.75 | 324 | 419 | 483 | 4.3 | 3.9 | 9.8 | 7.2 | 1.9 |
| 1.85 | 357 | 418 | 481 | 3.2 | 2.7 | 6.2 | 5.5 | 2.0 |
| 2.0# | 408 | 425 | 463 | 1.3 | 0.9 | 1.9 | 2.3 | 2.4 |

tively more porous than combustibles (Ronsse et al., 2013). Thus, lighter $SG_M$ coal has lower surface area due to low inorganic constraints, and with increase in $SG_M$ from 1.425 to heavier density fractions surface area reduces. The highest pore volumes and surface area for 1.425 $SG_M$ coal inferred the optimum combinations of inorganic matter and combustibles composition to yield highly porous coal.

## XRF of Coal

Fluctuations in inorganic oxides of different $SG_M$ coal's ash are obtained from XRF and are summarized in Table 4. Table 4 shows that 1.25 $SG_M$ coal had minimum content of $SiO_2$ (46.72%) and $Al_2O_3$ (24.30%) compared to other heavier $SG_M$ coals. $SiO_2$ and $Al_2O_3$ are alkaline with four coordination numbers and are major oxides of concern with respect to the slagging and fouling properties of coal. $Fe_2O_3$ and CaO are non-fluxing alkaline oxides with six co-ordination numbers. MgO is another alkaline earth metal oxide present in coal. Coal with 1.85 $SG_M$ had a higher amount of MgO, while 2.0 $SG_M$ coal contained higher quantities of $Fe_2O_3$ (10.12%) and CaO (14.97%). MnO, $Na_2O$, $K_2O$, $P_2O_5$ and $Cr_2O_3$ are basic oxides, and were in smaller quantities in all coal samples. The availability of different alkaline and basic oxides significantly affects the coal combustion properties by modifying the ash thickness characteristics as well as slagging and fouling tendencies. Slagging and fouling parameters such as base acid ratio ($R_{BA}$), fouling factor ($F_{IF}$) and silica ratio ($S_{RT}$) were estimated using inorganic oxides based on Eqs. (9)–(11) (García et al., 2015; Mishra et al. 2016b) and are summarized in Table 5.

$$R_{BA} = \frac{K_2O + Na_2O + Fe_2O_3 + MgO + CaO}{Al_2O_3 + SiO_2 + TiO_2} \quad (9)$$

$$F_{IF} = R_{BA} \times (K_2O + Na_2O) \quad (10)$$

$$S_{RT} = \frac{SiO_2}{SiO_2 + CaO + MgO + Fe_2O_3} \quad (11)$$

where $R_{BA}$ infers the ash slagging nature of coal, with higher value of $R_{BA}$ signifies higher slag formation nature on the boiler tubes. Theoretically, $R_{BA}$ value $< 0.5$ signifies mild ash deposition, 0.5–1 moderate ash deposition while $R_{BA} > 1$ indicates high deposition properties (García et al., 2015). $F_{IF} \leq 0.6$ signifies mild fouling characteristics, while 0.60–40 shows high fouling nature of coal (García et al., 2015). $S_{RT}$ is an indicator of slagging performance, and good coal having $S_{RT} > 0.78$ infers hard to fuse (Mishra et al., 2016b).

Table 5 presents the variations in $R_{BA}$, $F_{IF}$ and $S_{RT}$ for different $SG_M$ coals. Table 5 signifies that, as coal $SG_M$ increased from 1.25 to 2.0, $R_{BA}$ increased from 0.19 to 1.19 and $F_{IF}$ increased from 0.35 to 0.97, signifying that heavier $SG_M$ coals have higher slagging and fouling tendency. Similarly, $S_{RT}$ values of 1.85–2.0 $SG_M$ coal were very inferior compared to the permissible limit ($< 0.78$), signifying higher melting nature of heavier $SG_M$ coals. Overall, based on ash characterization, it can be concluded that 1.25 to 1.75 $SG_M$ coals can be utilized in thermal power plants.

### Impact of $SG_M$ on Combustion Characteristics

Combustion analysis for different $SG_M$ coal fractions was done under the oxygen ($O_2$) atmosphere using TGA–DTG investigation. Variations in mass loss (TGA) and mass loss rate (DTG) profiles with $SG_M$ of coal are shown in Figure 3. Figure 3a infers that all coal samples exhibit distinguished mass loss profiles according to functional groups, surface properties, hydrocarbons and mineral compositions present in individual coals. About 2–3% mass loss happened within 30–150 °C due to moisture evaporation from the coal texture. Later, some mass gain in 150–300 °C is seen, related to oxygen adsorption into coal porous surface texture. Further, a significant mass loss was found for all $SG_M$ coal fractions, inferring the initiation of combustion. Such significant mass loss is due to the release of lighter hydrocarbons and organic volatile matter due to the heating of coal, delivering the requisite energy to ignite the solid carbon available in the sample (Kumar and Nandi, 2022). Within 450–500 °C, a sharp mass loss was found, signifying that the rate of combustion was at its maximum in this temperature region. After that, the combustion rate was almost negligible, signifying the completion of the combustion process due to the total burnout of carbonaceous material available in coal. The DTG curve shown in Figure 3b comprehensively describes such mass loss profiles. The number of coal combustion characteristics parameters, such as $T_{IN}$, $T_{PK}$, $T_{FL}$ and $DTG_{peak}$ were extracted from TGA and are summarized in Table 6. Table 6 and Figure 3b show that the mass loss pattern of specific coal samples can be attributed to the combustion behavior of that coal samples. Coal with 1.25 $SG_M$ had the maximum mass loss rate (38.5 mass%/min) compared to the other heavier $SG_M$ coals. This infers that 1.25 $SG_M$ coal is most favorable for thermal utilities with superior combustion rate that can increase the steam generation rate due to maximum heat release rate. Such superior rate of mass loss of 1.25 $SG_M$ coal can be linked with the availability and non-availability of different functional groups in coal as discussed in section **Impact of SGM on FTIR**, inferring that 1.25 $SG_M$ coal has all kinds of combustible functional groups. However, the combustion rate is inferior for heavier density coals which can be attributed to weak peak or absence of different functional groups such as C=C tri-substituted alkenes (800–750 $cm^{-1}$), alkene (970–900 $cm^{-1}$), aliphatic chains of CH bending such as aldehyde and alkane (1500–1400 $cm^{-1}$), aliphatic–$CH_2$ and –$CH_3$ stretching (3000–2800 $cm^{-1}$) and alcoholic/prime amine group (3400–3350 $cm^{-1}$) as found from Table 2. These findings infer that coal consists of tri-substituted alkenes, aldehyde, alkane, alcoholic and prime amine groups with good combustion properties and exhibiting a better combustion rate. These functional groups in coal might be available as FC and VM, which play a crucial role during combustion. From Table 6, it is found that when coal $SG_M$ progressed from 1.275 to 2.0, $T_{IN}$ rose from 285 to 408 °C, $T_{PK}$ ranged from 398 to 425 °C, $T_{FL}$ varied from 469 to 497 °C. All such temperatures are on the higher side for 1.25 $SG_M$ coal. Such fluctuations may be attributed to the higher oxygen availability in 1.275 $SG_M$ coal (Table 1). Later, it was seen that $T_{IN}$ reduced with progress in $SG_M$ of coal. Such fluctuations of $T_{IN}$ are due to a decrease of VM with rise in coal $SG_M$ as VM promotes ease of ignition. Overall, it can be concluded that heavier $SG_M$ coal is more difficult to ignite. The impact of $SG_M$ of coal on different performance indices, namely, $I_{IN}$, $C_{IN}$, $B_{IN}$ and $H_{IN}$ are evaluated using Eqs. (1)–(4), and are summarized in Table 6. Ignition index ($I_{IN}$) value should be higher as it infers the ignition properties of coal (Aich et al., 2019). Characteristics index ($C_{IN}$) should be higher as it indicates the combustion behavior of coal (Xinjie et al., 2021). Burnout index ($B_{IN}$) shows the reactivity state between coal and air/oxygen. A higher $B_{IN}$ value indicates improved combustion reactivity and adequate energy release to sustain the combustion process (Kumar and Nandi, 2022). However, the heat intensity index ($H_{IN}$) represents combustion stability and the smaller value represents superior combustion characteristics (Aich et al., 2019). Table 6 shows that $I_{IN}$ reduced from 38.1 to 0.9 mass/min$^3$ as $SG_M$ of coal increased from 1.25 to 2.0, indicating ignition difficulty increases with increase in $SG_M$. Such ignition problems may be due to reduced hydrogen and VM content in coal for higher $SG_M$ coals. Similarly, $C_{IN}$ degraded from 101.1 to 1.9 mass$^2$/min$^2$ $^{\circ}C^3$ as $SG_M$ of coal increased from 1.25 to 2.0, representing difficulty in combustion with increase in $SG_M$. Further, with the progression of SGM from 1.25 to 2.0, $B_{IN}$ reduced from 76.4 to 2.3 mass/min$^4$, signifying that high $SG_M$ coal requires more time for complete combustion. Overall, it can be summarized that 1.25–1.55 $SG_M$ coals show better combustion properties compared to other heavier $SG_M$ coals. $H_{IN}$ values enhanced from 0.9 to 2.4 °C, with the highest value of 2.4 °C for 2.0 $SG_M$ coal. This indicates that 2.0 $SG_M$ coal has poor combustion performance compared to other $SG_M$ coals. Overall, the analysis of performance indices and burning profile parameters convey that the combustion characteristics of 1.325–1.55 $SG_M$ coal are superior to other $SG_M$ coals.

## Impact of $SG_M$ on Coal Utilization

Coal coming to thermal utilities must have sufficient heat release rates to keep the combustor temperature at the optimum level. In this context, heat release rate ($R_H$, kcal/min) and minimum burning duration ($D_M$, min) for a unit quantity of coal were calculated based on HHV and maximum combustion rate ($DTG_{Peak}$) of coal using the following equations (Kumar and Nandi, 2022):

$$R_H = \frac{HHV \times DTG_{Peak}}{100} = \frac{kcal}{kg} \times \frac{kg}{100 \times min} = kcal/min \quad (12)$$

$$D_M = \frac{1gm}{\frac{DTG_{Peak}}{100} \times \frac{gm}{min}} = \frac{100}{DTG_{Peak}} min \quad (13)$$

In the pulverized combustion chamber, the entire range of coal particles have an equal duration to burn. This burning duration depends on coal's turbulence and settling velocity in the combustion chamber. All the coal particles must be burnt before coming outside the combustor as a bottom ash. With variation of chemical and physical properties of coal, the particles might not burn out in a timely manner. In such conditions, $D_M$ could act as a key parameter in determining how effectively coal burns. Theoretically, $D_M$ is the minimum time duration for total burnout of any coal particles. Similarly, $R_H$ is the maximal heat release rate associated with produced steam quality. Figure 4 represents the fluctuations of $D_M$ and $R_H$ with the variation in $SG_M$ of coal. It is observed from Figure 4 that, with variation in $SG_M$ of coal from 1.25 to 2.0, $D_M$ ranged from 3 to 75 min while $R_H$ ranged from 3292 to 19.1 kcal/min. Coal with 1.25 $SG_M$ showed the maximum $R_H$ (3292 kcal/min) and minimum $D_M$ (3 min). Similarly, a minimum $R_H$ of 19.1 kcal/min was seen for 2.0 $SG_M$ with maximum $D_M$ (75 min). This observation infers that heavier $SG_M$ coal requires longer duration for complete combustion than lighter $SG_M$ coals. Such fluctuation in $R_H$ and $D_M$ are attributed to the increase in mineral matter and decline in combustible matter present in coal with increase in $SG_M$. Higher ash thickness associated with increased mineral matter creates obstacles for the diffusion of $O_2$, $CO_2$, etc. gases, and consequently, the combustion rate deteriorates.

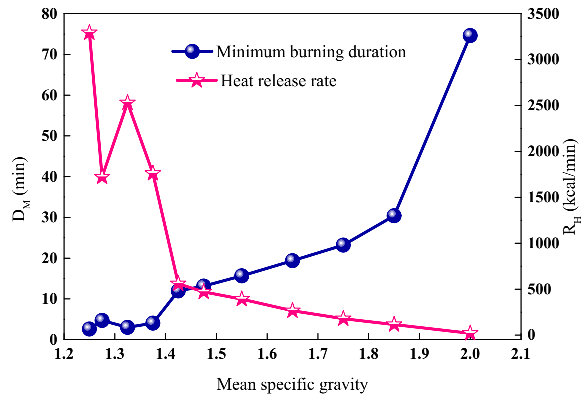


**Figure 4.** Fluctuations of heat release rate and burning duration with coal $SG_M$..

Thus, selecting coal with the optimum $SG_M$ to run a combustor efficiently is very important. Overall, it can be concluded that coals with 1.25 to 1.55 $SG_M$ infer better heat release rate with lower combustion duration than 2.0 $SG_M$ coal.

## Impact of $SG_M$ on Coal Feed Rate and Ash Generation Rate

As discussed in the previous section (Impact of SGM on Coal Utilization), the rate of heat release ($R_H$, kcal/min) substantially fluctuated with $SG_M$ of coal and depended on HHV, ash content and $DTG_{Peak}$. Due to fluctuations in ash, HHV, combustion rate and $R_H$, the required coal feed and corresponding ash generation rate for constant energy output also significantly deviated as thermal power plants are required to combust different amounts of coal to sustain uniform electricity production (Kumar and Nandi, 2022). Coal feed rate ($W_{Fuel}$) and ash generation rate ($W_{ash}$) for 10000 kcal heat generation were calculated respectively using the following equations (Kumar and Nandi, 2022):

$$W_{Fuel} = \frac{10000}{HHV} \quad (14)$$

$$W_{ash} = \frac{W_{Fuel} \times Ash(\%)}{100} \quad (15)$$

Variations in $W_{Fuel}$ and $W_{ash}$ with variation in $SG_M$ of coal is shown in Figure 5. Figure 5 shows that coal consumption increased from 1.17 to 7.03 kg as coal $SG_M$ rose from 1.25 to 2.0. This rise of coal consumption is due to the reduction of HHV with $SG_M$ of coal. Ash generation rate also significantly increased from 0.03 to 5.37 kg as $SG_M$ of coal increased.

Such observations for thermal power plants infer that it is important to use coal with needed combustion characteristics with lower ash content and higher HHV. Based on the lower coal consumption and ash generation rates, 1.25 to 1.55 $SG_M$ coal should be used in thermal power plants.

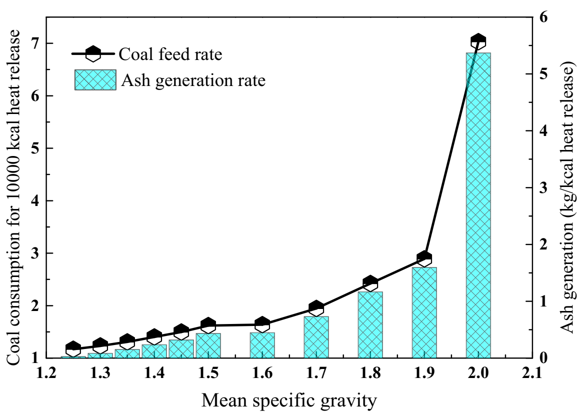


**Figure 5.** Fluctuations of $W_{Fuel}$ and $W_{ash}$ with coal $SG_M$..

## Impact of $SG_M$ on Coal Combustion Kinetics

Fluctuation of activation energy ($E_C$) and pre-exponential factor (*f*) for different $SG_M$ coal were determined using Eq. (5) and are shown in Figure 6. From Figure 6a, it is clear that, with increase in $SG_M$ from 1.25 to 2.0, $E_C$ reduced from 121.81 to 54.60 kJ/mol. The minimum $E_C$ was found for 1.65 $SG_M$ coal and maximum $E_C$ for 1.25 $SG_M$ coal. Such fluctuation in $E_C$ with $SG_M$ may be attributed to changes in surface characteristics and availability of functional groups. For 1.65 $SG_M$ coal, almost all kinds of functional groups are available, excluding only the aldehyde group at 1500–1400 $cm^{-1}$. For 1.25 $SG_M$ coal, surface area and pore volume were inferior, and functional groups such as tri-substituted alkenes (800–750 $cm^{-1}$), alkenes (970–900 $cm^{-1}$), aliphatic chains of C–H bending (1500–1400 $cm^{-1}$) and alcoholic group (3700–3650 $cm^{-1}$) are either weakly present or absent as mentioned in Table 2. Figure 6b shows that *f* increased from $1.96 \times 10^4$ $sec^{-1}$ to $21.23 \times 10^4$ $sec^{-1}$ as $SG_M$ progressed from 1.25 to 2.0, inferring the lowest combustion reactivity of lighter $SG_M$ coal compared to other heavier $SG_M$ coal. Such fluctuation in *f* with $SG_M$ is due to deviation of different functional groups availability in individual coal. However, the highest *f* was observed for 1.65 $SG_M$ coal and the lowest for 1.25 $SG_M$ coal.

For coal with 1.65 $SG_M$, surface properties were good and almost all functional groups were available, excluding only the aldehyde group at 1500–1400 $cm^{-1}$. For coal with 1.25 $SG_M$, surface characteristics were inferior, and most of the functional

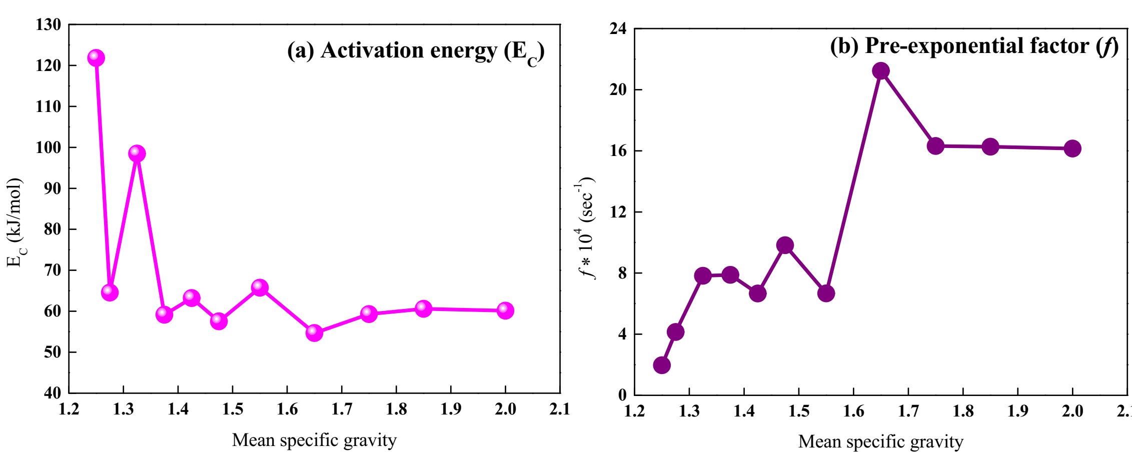


**Figure 6.** Fluctuations of (**a**) $E_C$ and (**b**) *f* with coal $SG_M$..

groups, such as alkenes, tri-substituted alkenes, aldehyde and alcoholic groups were absent or weakly present. Such observations infer that, for better combustion characteristics with minimum $E_C$ and maximum *f*, almost all of the functional groups should be available in coal.

## Impact of $SG_M$ on Thermodynamic Parameters

Variations in enthalpy (ΔH), Gibbs free energy (ΔG) and entropy (ΔS) with coal $SG_M$ were evaluated using Eqs. (6)–(8) and are shown in Figure 7. ΔH infers reaction behavior (exothermic/endothermic) during coal combustion. The higher ΔH value signifies more heat input is needed during the coal combustion (Mishra and Mohanty, 2020). From Figure 7a it can be noticed that, with increase in $SG_M$ from 1.25 to 2.0, ΔH reduced from 116.80 to 48.93 kJ/mol. A lower ΔH value was seen for 1.65 $SG_M$ coal, while the highest ΔH for 1.25 $SG_M$ coal, signifying that less endothermic energy is needed for 1.65 SGM coal than other coals. Such variations in ΔH with $SG_M$ may be due to variations in functional groups' availability. For coal with 1.65 $SG_M$, most functional groups were available, excluding only the aliphatic chain of C–H bending between 1500 and 1400 $cm^{-1}$ wavelength. Whereas for coal with 1.25 $SG_M$, large number of functional groups such as C=C tri-substituted alkenes (800–750 $cm^{-1}$), alkene (970–900 $cm^{-1}$), aldehyde (1500–1400 $cm^{-1}$), alkane (3000–2800 $cm^{-1}$) and alcoholic/prime amine group (3400–3350 $cm^{-1}$) were either weakly present or absent as shown in Table 2. ΔG signifies the decomposition difficulty of coal combustion. The higher ΔG value indicates that more decomposition energy is needed during the reaction (Dhyani et al., 2017). Figure 7b shows that ΔG value of 1.25 $SG_M$ coal was maximum (238.54 kJ/mol) compared to other coals, signifying more decomposition energy is needed for

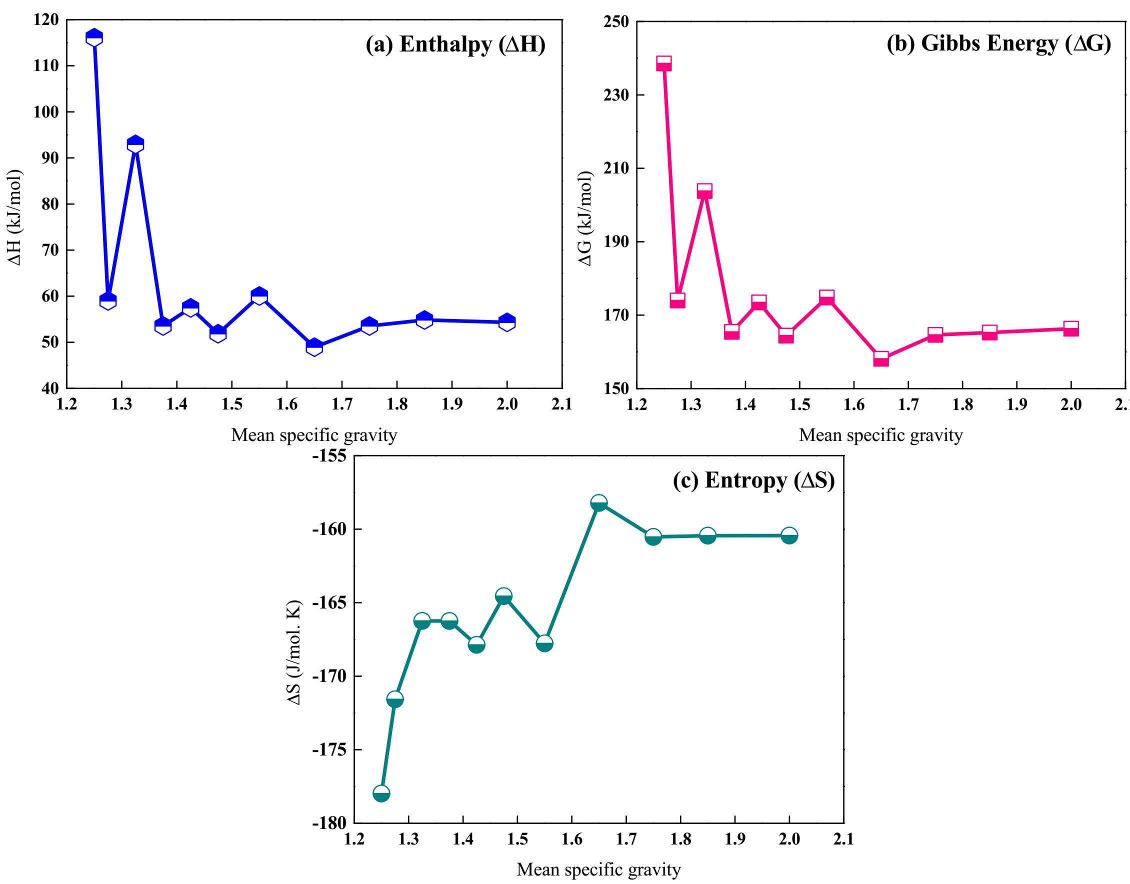


**Figure 7.** Variation in (**a**) ΔH, (**b**) ΔG and (**c**) ΔS with coal $SG_M$..

1.25 $SG_M$ coal. Such observation may be due to lower surface characteristics and unavailability of combustible functional groups such as tri-substituted alkenes, aldehyde, alcoholic and prime amine groups. However, ΔG value was the lowest for 1.65 $SG_M$ coal, which may be due to good surface characteristics and the presence of almost all functional groups except the aldehyde group. ΔS value should be higher as it represents coal combustion reactivity (Aprianti et al., 2023). From Figure 7c, ΔS value was lowest (– 177.98 J/mol. K) for 1.25 $SG_M$ coal and highest (– 158.22 J/mol. K) for 1.65 $SG_M$ coal. Such observation infers that the combustion reactivity of 1.65 $SG_M$ coal is superior to other coal fractions. Overall, thermodynamic analysis indicates that, for best-suited combustion characteristics with lower ΔH, ΔG and maximum ΔS, most functional groups and higher surface properties should be present in coal.

## CONCLUSIONS

Different $SG_M$ fractions of coal were generated using the float–sink experiments. Characterization results signified that, when $SG_M$ of coal rose from 1.25 to 2.0, ash deteriorated from 2.41 to 76.36%, carbon reduced from 79.64 to 53.65% and HHV declined from 9606 to 6577 kcal/kg. Ash analysis inferred that heavier $SG_M$ coals have higher slagging and fouling characteristics. FTIR provided insight into coal combustion characteristics and distribution of hydrocarbons with $SG_M$. The combustion rate of 1.25 $SG_M$ coal was found higher due to stronger or moderate availability of most of the hydrocarbons such as alkane, alkene, aldehyde and alcoholic as well as aliphatic C–H stretching and aromatic nucleus of C=C as obtained from FTIR. Combustion experiments showed that, with progression of coal $SG_M$ from 1.25 to 2.0, $T_{IN}$ rose from 285 to 408 °C, $T_{PK}$ ranged from 398 to 425 °C, and $T_{FL}$ varied from 469 to 497 °C. The kinetic analysis signified that activation energy ranged from 121.81 to 54.60 kJ/mol as $SG_M$ of coal varied from 1.25 to 2.0. Thermodynamic analysis inferred that 1.65 $SG_M$ coal has a lower value of ΔH (48.93 kJ/mol) and ΔG (158.09 kJ/mol), inferring smooth decomposition during the coal combustion. Overall, the theoretical and experimental analysis suggested that 1.325 to 1.55 $SG_M$ would be preferable for thermal power plants. This work thus observed variations in coal combustion characteristics with its mean specific gravity ($SG_M$).

## DATA AVAILABILITY

All the data generated or analyzed during this study are included in this article.

## DECLARATIONS

**COMPETING INTEREST** The authors declare that they have no known competing financial interests or personal relationships that could have appeared to influence the work reported in this paper.

## REFERENCES


Aich, S., Nandi, B. K., & Bhattacharya, S. (2019). Utilization of Sal leaves and Sal leaves char to improve the combustion performance of reject coal. *Energy Sources, Part A Recovery, Utilization and Environmental Effect, 41*(19), 2299–2312.

Aprianti, N., Faizal, M., Said, M., Nasir, S., & Fudholi, A. (2023). Gasification kinetic and thermodynamic parameters of fine coal using thermogravimetric analysis. *Energy, 268*, 126666.

Banerjee, A., Mishra, P. R., Mohanty, A., Chakravarty, K., Biswas, R. D., Sahu, R., & Chakravarty, S. (2016). Distribution of mineral species in different coal seams of Talcher coalfield and its transformation behaviour at varying temperatures. *International Journal of Coal Science and Technology, 3*, 97–103.

Biswas, S., Choudhury, N., Sarkar, P., Mukherjee, A., Sahu, S. G., Boral, P., & Choudhury, A. (2006). Studies on the combustion behaviour of blends of Indian coals by TGA and drop tube furnace. *Fuel Processing Technology, 87*, 191–199.

Cai, J., Yang, S., Zheng, W., & Song, W. (2021). Risk assessment of oxidizability of coal after dynamic hazard and its effect on functional groups and radicals. *Natural Resources Research, 30*(6), 4533–4545.

Cao, W., Cao, W., Peng, Y., Qiu, S., Miao, N., & Pan., F. (2015). Experimental study on the combustion sensitivity parameters and pre-combusted changes in functional groups of lignite coal dust. *Powder Technology, 283*, 512–518.

Chakraborty, P., Hazra, B., Sarkar, P., Singh, A. K., Singh, P. K., & Kumar, S. (2021). Thermal behavior of some Indian coals: Inferences from simultaneous thermogravimetric-calorimetry and rock-eval. *Natural Resources Research, 30*(3), 2161–2177.

Chakravarty, S., Chakravarty, K., Mishra, V., Chakladar, S., Mohanty, A., & Sharma, M. (2020). Characterization of chemical structure with relative density of three different ranks of coal from India. *Natural Resource Research, 29*(5), 3121–3136.

Dhyani, V., Kumar, J., & Bhaskar, T. (2017). Thermal decomposition kinetics of sorghum straw via thermogravimetric analysis. *Bioresource Technology, 245*, 1122–1129.

Fang, X., Cai, Y., Hu, Q., Liu, Q., Gao, P., Qian, Y., & Jia, Q. (2022). Hydrocarbon retention and its effect on pore structure evolution of marine shale based on pyrolysis simulation experiments. *Energy and Fuels, 36*, 13556–13569.

Fortish, D., Essenhigh, R. H., Froberg, R. W., Schnell, U., & Hein, K. R. G. (2000). Influence of the density profile on the combustion characteristics of carbon: A theoretical study. *Proceedings of the Combustion Institute, 28*, 2251–2260.

García, R., Pizarro, C., Álvarez, A., Lavín, A. G., & Bueno, J. L. (2015). Study of biomass combustion biomass combustion wastes. *Fuel, 148*, 152–159.

Gupta, O. P. (2000). *Elements of fuels, furnaces and refractories* (5th ed.). Khanna publishers.

Gupta, R. (2007). Advanced coal characterization: A review. *Energy and Fuels, 21*, 451–460.

Kumar, P., & Nandi, B. K. (2021). Combustion characteristics of high ash Indian coal, wheat straw, wheat husk and their blends. *Material Science for Energy Technologies, 4*, 274–281.

Kumar, P., & Nandi, B. K. (2022). Effect of rice husk blending on combustion characteristics of high ash Indian coal analyzed in TGA. *International Journal of Coal Preparation and Utilization, 42*(12), 3698–3711.

Kumari, S., Gouricharan, T., Pandey, J. K., Udayabhanu, G., & Sharma, S. N. (2016). Evaluation of quartz reduction by coal cleaning for thermal utilization of an Indian coal. *International Journal of Coal Preparation and Utilization, 38*, 53–63.

Liu, Z., Liu, S., Shi, R., Wang, J., Xie, M., & Zheng, S. (2020). A control strategy of the air flow rate of coal-fired utility boilers based on the load demand. *ACS Omega, 5*, 31199–31208.

Lv, B., Luo, Z., Fu, Y., Zhang, B., Qin, X., & Zhu, X. (2020). Particle mixing behavior of fine coal in density control of gas–solid separation fluidized bed. *Particuology, 50*, 76–87.

Merdun, H., & Laouge, Z. B. (2021). Kinetic and thermodynamic analyses during co-pyrolysis of greenhouse wastes and coal by TGA. *Renewable Energy, 163*, 453–464.

Mishra, D. P. (2022). Effects of intrinsic properties, particle size and specific surface area on WOP and spontaneous combustion susceptibility of coal. *Advanced Powder Technology, 33*, 103454.

Mishra, R. K., & Mohnaty, K. (2020). Kinetic analysis and pyrolysis behaviour of waste biomass towards its bioenergy potential. *Bioresource Technology, 311*, 123480.

Mishra, V., Sharma, M., Chakravarty, S., & Banerjee, A. (2016a). Changes in organic structure and mineral phases transformation of coal during heat treatment on laboratory scale. *International Journal of Coal Science and Technology, 3*(4), 418–428.

Mishra, V., Bhowmick, T., Chakravarty, S., Varma, A. K., & Sharma, M. (2016b). Influence of coal quality on combustion beahviour and mineral phases transformations. *Fuel, 186*, 443–455.

Nag, P. K. (2014). *Power plant engineering* (4th ed.). New Delhi: McGraw Hill Education Private Limited.

Nyoni, B., Duma, S., Shabangu, S. V., & Hlangothi, S. P. (2020). Comparison of the slow pyrolysis behavior and kinetics of coal, wood and algae at high heating rates. *Natural Resources Research, 29*(6), 3943–3955.

Odeh, A. O. (2015). Qualitative and quantitative ATR-FTIR analysis and its application on coal char to of different ranks. *Journal of Fuel Chemistry and Technology, 43*, 129–137.

Raghuvanshi, G., Chakraborty, P., Hazra, B., Adak, A. K., Singh, P. K., Singh, A. K., & Singh, V. (2022). Pyrolysis and combustion behavior of few high-ash Indian coals. *International Journal of Coal Preparation and Utilization, 42*(8), 2452–2472.

Ronsse, F., Hecke, S. V., Dickinson, D., & Prins, W. (2013). Production and characterization of slow pyrolysis biochar: Influence of feedstock type and pyrolysis conditions. *Global Change Biology: Bioenergy, 5*, 104–115.

Saini, M. K., & Srivastava, P. K. (2017). Effect of coal cleaning on ash composition and its fusion characteristics for a high-ash non-coking coal of India. *International Journal of Coal Preparation and Utilization, 37*(1), 1–11.

Sampath, K. H. S. M., Sin, I., Perera, M. S. A., Matthai, S. K., Ranjith, P. G., & Dong-yin, L. (2020). Effect of supercritical-$CO_2$ interaction time on the alterations in coal pore structure. *Journal of Natural Gas Science and Engineering, 76*, 103214.

Sarkar, P., Mukherjee, A., Sahu, S. G., Choudhury, A., Adak, A. K., Kumar, M., Choudhury, N., & Biswas, S. (2013). Evaluation of combustion characteristics in thermogravimetric analyzer and drop tube furnace for Indian coal blends. *Applied Thermal Engineering, 60*, 145–151.

Shen, J., Liu, J., Xing, Y., Zhang, H., Luo, L., & Jiang, X. (2018). Application of TG-FTIR analysis to superfine pulverized coal. *Journal of Analytical and Applied Pyrolysis, 133*, 154–161.

Song, H., Liu, G., Zhang, J., & Wu, J. (2017). Pyrolysis characteristics and kinetics of low rank coals by TG-FTIR method. *Fuel Processing Technology, 156*, 454–460.

Sun, K., Kang, M., Zhang, Z., Jin, J., Wang, Z., Pan, Z., Xu, D., Wu, F., & Xing, B. (2013). Impact of deashing treatment on biochar structural properties and potential sorption mechanisms of phenanthrene. *Environmental Science and Technology, 47*, 11473–11481.

Tiwari, R., Bhattacharya, S., & Raghav, P. (2015). A discussion on non-coking coal pricing systems adopted in different countries. *Vikalpa: The Journal for decision Makers, 40*(1), 62–73.

Wang, G., Zhang, J., Shao, J., Liu, Z., Zhang, G., Xu, T., Guo, J., Wang, H., Xu, R., & Lin, H. (2016). Thermal behavior and kinetic analysis of co-combustion of waste biomass/low rank coal blends. *Energy Conversion and Management, 124*, 414–426.

Wang, P., Wang, G., Zhang, J., Lee, J. Y., Li, Y., & Wang, C. (2018). Co-combustion characteristics and kinetic study of anthracite coal and palm kernel shell char. *Applied Thermal Engineering, 143*, 736–745.

Wang, H., Li, J., Fan, C., Wang, L., & Chen, X. (2022). Thermal kinetics of coal spontaneous combustion based on multiphase fully coupled fluid-mechanical porous media model. *Natural Resources Research, 31*(5), 2819–2837.

Wu, D., Zhou, P., Yan, H., Shi, P., & Zhou, C. Q. (2019). Numerical investigation of the effects of size segregation on pulverized coal combustion in a blast furnace. *Powder Technology, 342*, 41–53.

Xinjie, L., Singh, S., Yang, H., Wu, C., & Zhang, S. (2021). A thermogravimetric assessment of the tri-combustion process for coal, biomass and polyethylene. *Fuel, 287*, 119355.

Xuguang, S. (2005). The investigation of chemical structure of coal macerals via transmitted-light FT-IR microspectroscopy. *Spectrochim Acta A, 62*, 557–564.

Yu, Z., Zhang, X., Wen, Y., Haihui, X., Sherong, H., & Yu, S. (2020). Pore structure and its impact on susceptibility to coal spontaneous combustion based on multiscale and multifractal analysis. *Scientific Reports, 10*, 7125.

Zhang, W., Jiang, S., Wang, K., Wang, L., Xu, Y., Wu, Z., & Shao, H. (2015). Thermo gravimetric dynamics and FTIR analysis on oxidation properties of low-rank coal at low and moderate temperatures. *International Journal of Coal Preparation and Utilization, 35*, 39–50.

Zou, L., Yang, W., Zhao, Q., Ma, L., Ren, L., & Wang, Y. (2022). Research on self-ignition characteristics and prediction indices of pulverized low-rank coal under different oxygen concentrations. *Natural Resources Research, 31*(2), 897–911.